

BEHAVIOR OF LIGHT- WEIGHT CONCRETE SOLID SLABS REINFORCED USING G.F.R.P. REBAR

¹Alaa G. Sherif, ²Nasr Z. Hassan, ³Mohamed Saber, ⁴Mirhan W. Adly

¹ Prof. of Concrete Structures, Faculty of Eng., Mattaria, Helwan Univ., Cairo, Egypt

² Assoc. Prof. of Concrete Structures, Faculty of Eng., Mattaria, Helwan Univ., Cairo, Egypt

³Teacher, Construction Engineering Dept., Egyptian Russian University, Cairo, Egypt

⁴Teaching Assistant, Construction Engineering Dept., Egyptian Russian University, Cairo, Egypt

Abstract: Deterioration of concrete structures throughout the world and the cost of their repair and rehabilitation have become a major concern to engineer and researchers in recent years. Almost cases the repair costs can be twice or more of the original cost. For example, in Canada, it is estimated that the cost of repair of parking garages is in the range of 6 billion dollars, and over 74 billion dollars for all concrete structures. The estimated repair cost for existing highway bridges in the USA is over 50 billion dollars, and 1-3 trillion dollars for all concrete structures. In Europe, steel corrosion has been estimated to cost about 3 billion dollars' year. Excessive corrosion problem also exists in Arabian Gulf countries (Benmokrane et al., 1998). Organizations, private industry and university researchers are seeking ways to avoid the corrosion problem and thereby eliminate, partially or totally, burden of never ending repair costs. One preferred solution, which has assumed the status of cutting edge research in many industrialized countries, is the use of fiber reinforced polymer (FRP) rebars in concrete.

FRP reinforcement has an advantage over steel in that it has high corrosion resistance and a high strength to weight ratio, thus for structures built in or close to seawater or at similar corrosive environment. They are also non-conductive for electricity and non-magnetic.

Keywords: Solid plates, Flexure strength, GFRP rebar, Crack pattern.

1. INTRODUCTION

In this study, details of the experimental program consisting of testing 12 full scale concrete slabs subjected to moment loading is are presented. The main objectives of the experimental program are: 1) to investigate the behavior of using steel and GFRP bars to enhance the moment strength of reinforced concrete slabs. 2) to optimize the GFRP bars ratio that leads to the ultimate load carrying capacity. 3) To compare between different reinforcement steel and GFRP bars as a main reinforcement in behavior on type of load of light weight concrete slabs one and two way. 4) To address the deformation and ductility behavior of light weight concrete slabs having steel and GFRP bars. 5) To studding behavior of light weight concrete with steel and GFRP bars as a main reinforcement.

2. EXPERMINTAL STUDY

The tested specimens were categorized into two groups as shown in Table 1. The first group (Group I) as a one-way slabs had six slabs. Three slabs were reinforced by steel and other three slabs reinforced by GFRP with different ratio of reinforcement. The results of the first three specimens of the Group-I were meant to be the reference for the results of the other specimens. The second group (Group II) has the same parameter of group but with different dimension as a two-way slab. Results of specimens this Groups I,II were used to understand the behavior of concrete slabs having fiber. The slabs in these groups were tested under monotonic load condition. They had different reinforcement ratio with different dimensions of the slab. Table 3.1 summarizes the geometric characteristics of all tested specimens.

Our experimental program included Group I, II reinforced with Steel & GFRP bars.

Name of specimens wrote as: Sx-y

Where S: Slab.

X: number of group.

Y: number of specimens.

TABLE (I): Specimen Details

| Group | Slab No. | No. of RFT (bars) | Diameter (mm) | Material | Surface Texture | Slab Type | Type of Load | Dimensions (mm) |
|-------|----------|-------------------|---------------|----------|-----------------|-----------|--------------|-----------------|
| I | S1-1 | 8 | 8 | steel | Smooth | One way | Distribution | 2000*1000*100 |
| | S1-2 | 5 | 10 | steel | Ribbed | One way | Distribution | 2000*1000*100 |
| | S1-3 | 10 | 10 | steel | Ribbed | One way | Distribution | 2000*1000*100 |
| | S1-4 | 8 | 8 | GFRP | Smooth | One way | Distribution | 2000*1000*100 |
| | S1-5 | 5 | 10 | GFRP | Ribbed | One way | Distribution | 2000*1000*100 |
| | S1-6 | 10 | 10 | GFRP | Ribbed | One way | Distribution | 2000*1000*100 |
| II | S2-1 | 8 | 8 | steel | Smooth | Two way | Distribution | 1700*1700*100 |
| | S2-2 | 5 | 10 | steel | Ribbed | Two way | Distribution | 1700*1700*100 |
| | S2-3 | 10 | 10 | steel | Ribbed | Two way | Distribution | 1700*1700*100 |
| | S2-4 | 8 | 8 | GFRP | Smooth | Two way | Distribution | 1700*1700*100 |
| | S2-5 | 5 | 10 | GFRP | Ribbed | Two way | Distribution | 1700*1700*100 |
| | S2-6 | 10 | 10 | GFRP | Ribbed | Two way | Distribution | 2000*1800*100 |

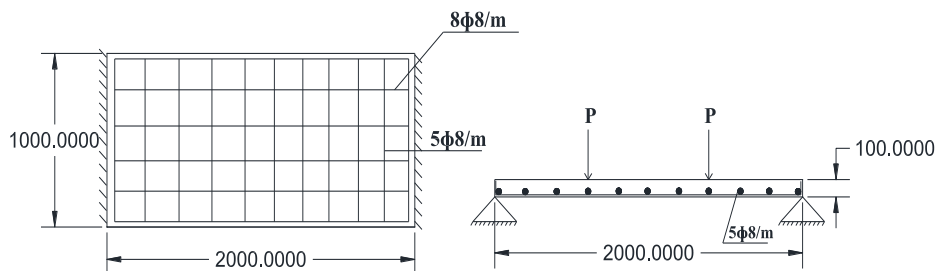


Fig 1: Reinforcement and Concrete Dimensions of Slab S1-1

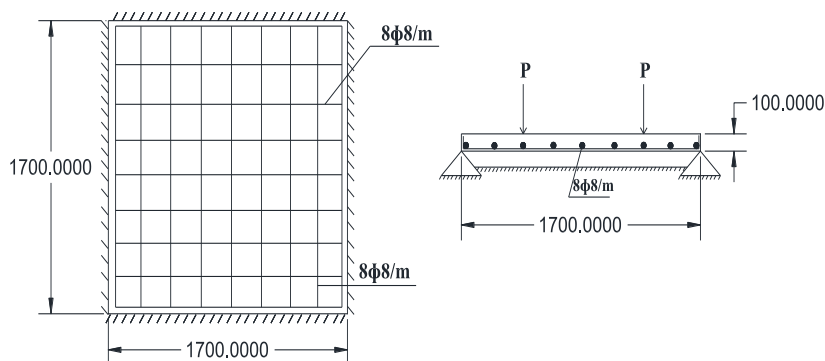


Fig 2: Reinforcement and Concrete Dimensions of Slab S2-1

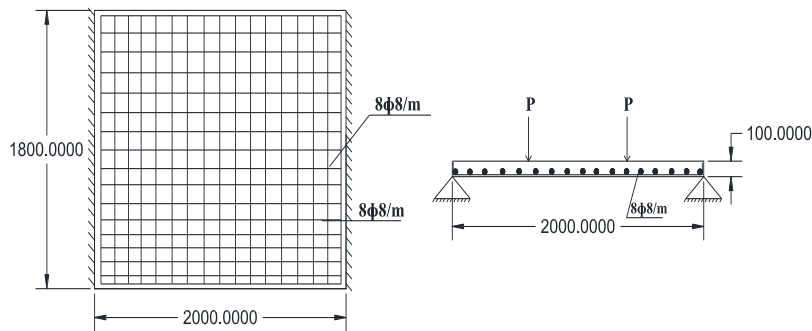


Fig 3: Reinforcement and Concrete Dimensions of Slab S3-1

2.1 Slab Modeling:

The tested specimens in the experimental program represented full scale prototype for building slabs. The dimensions of the tested specimens were chosen to represent one and two way slabs. Typically, the contra flexure points of a slab subjected to gravity state of loading are located at distance $0.5L$ from the center line, where L is the spacing between two supports Figure 4 shows the location of flexure points of a typical concrete slab subjected to gravity loads in a residential building. Accordingly, the tested specimens were 100 mm in thickness and 17000x17000 mm and 2000x1000 dimension.

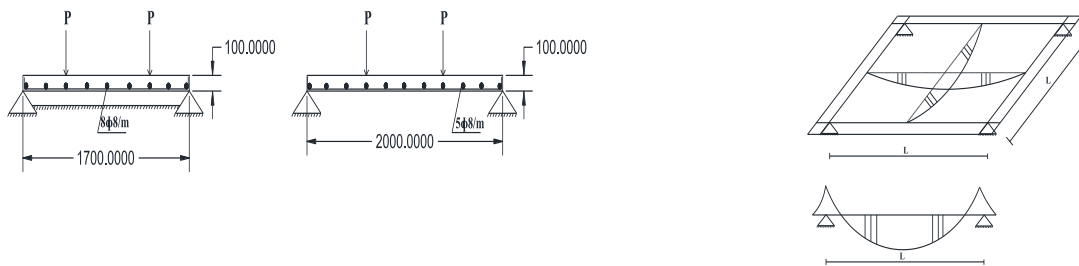


Fig 4: The location of flexure point and details of reinforcement

Figures 5 show typical steel reinforcement mesh of the tested specimens. This reinforcement is shown for the Slab of group I as a representative example. The twelve slabs have the same reinforcement mesh by different in type of reinforcement, as shown in Figure (5). The same configuration was used in all the tested slabs. As example for slab S1-1 The layer of the mesh had 11 deformed bars of diameter 8 mm at 200mm spacing in 2000mm direction and 9 deformed bars of diameter 8 mm at 100mm spacing in 1000 direction. The steel reinforcement ratio was chosen to ensure that the flexure capacity of the slab covered all cases.



Fig 5: Reinforcement layout of Slabs of Group I

2.1 Materials:

2.1.1 Concrete Mix Design

TABLE (2): Summary of Mix Design

| | | | |
|--|------------------------|--------------------------|-----------------------|
| fcu | 250 kg/m ² | Water | 139 L/m ³ |
| Max Slump | 100mm | Cement | 450 kg/m ³ |
| Min Slump | 50 mm | Coarse Aggregate | 630 kg/m ³ |
| Max Aggregate Size | 25 mm | Silica Fume | 40 kg/m ³ |
| Water Cement Ratio | 0.31 | Poly Foam | 330 L/m ³ |
| Concrete Type | Lightweight | Super Plasticizer | 13.5 L/m ³ |
| Unit Weight of Coarse Aggregate | 1500 kg/m ³ | Fine Aggregate | 630 kg/m ³ |

2.1.2 Light weight concrete Compressive Strength

Light weight concrete cubes (15x15x15 cm) were tested in the laboratory after 28 days using the compression universal machine. The universal machine is shown in Figure 6. The average light weight concrete cubic compressive strength and density of cubes are shown in Table (3) for different concrete batches to achieve properties of light weight concrete. From the table, it was obvious that light weight concrete reach to compressive strength 250Kg/cm² and density of it not increase more than 2000 Kg/m³



Fig 6: Universal Machine and tested cubes

TABLE (3) : Test Result of Cube Strength.

| Group No. | Cube No. | Strength (Kg/cm ²) | Average | Density (Kg/m ³) |
|-----------|----------|--------------------------------|---------|------------------------------|
| I | Cube 1 | 257 | 250.5 | 1946 |
| | Cube 2 | 245 | | 1936 |
| | Cube 3 | 236 | | 1966 |
| | Cube 4 | 280 | | 1992 |
| | Cube 5 | 235 | | 1983 |
| | Cube 6 | 256 | | 1933 |
| | Cube 7 | 245 | | 1922 |
| | Cube 8 | 250 | | 1900 |

| | | | | |
|-----------|----------------|-----|-------|------|
| II | Cube 9 | 282 | 245.5 | 1942 |
| | Cube 10 | 257 | | 1933 |
| | Cube 11 | 234 | | 1892 |
| | Cube 12 | 247 | | 1937 |
| | Cube 13 | 280 | | 1892 |
| | Cube 14 | 230 | | 1906 |
| | Cube 15 | 222 | | 1937 |
| | Cube 16 | 195 | | 1820 |

2.1.3 Casting and Compaction

The internal surfaces of the wood forms were covered with a polyethylene layer before pouring the concrete. Then the reinforcement meshes were placed in their place. The strain gauges were finally fixed at their specific locations on the reinforcement rebars. Figure 7 show the reinforcement details and the steps of casting the concrete. In the figure, the strain gauges' locations are shown. Finally, the concrete was compacted using a vibrator. The slab thickness was limited to 100 mm. eight test cubs of 15 cm side length were taken and tested. The test molds for cubes were coated with oil before casting. Then concrete was placed and mixing on three layers. Each layer was compacted using a standard rod with 25 blows. then tested to measure the concrete compressive strength after 28 days. The objective was to measure the exact concrete tensile/compressive strength of the specimens in the testing day



Fig 7: Reinforcement and Concrete Dimensions of Slabs

2.1.4 Curing

After the molds and forms were compacted, the specimens were covered with wet burlap for 48 hours. The slabs were then cured by emerging the surfaces using water. The cubes samples were totally submerged in water until testing. all samples were tested after 28 days. This meant to measure the exact concrete compressive strength in the same day of testing, Figures 8 show the curing of concrete.



Fig 8: Curing the concrete

2.2 Instruments

2.2.1 Deflection Measurements

Three dial gauges were used to record vertical deflection of the slabs at various locations. The gauges were installed on the bottom surface of slab. Two gauges were attached on edges of slabs at $L/2$ from center of slab in each direction. Another one gauge was installed at the mid-point of the slab. Figure 9 shows the three locations of the strain gauges of the Specimen S1-1 as an example.



Fig 9: Reinforcement and Concrete Dimensions of Slab S3-1

2.2.2 Strain Measurements

Before casting the slabs, electric resistance gauge (10mm length, 120 ohms' resistance with gauge factor of 2.10) were mounted and glued to the reinforcement. The locations of the strain gauge are shown in Figure 3.17. The steel strain was measured and recorded using a digital strain meter device (Figure 10). The strain meter was connected to the strain gauges using wires and the readings were recorded at each load increment.



Fig 10: Installation of the Strain Gauges to the Steel and GFRP Reinforcement

3. EXPERIMENTAL RESULTS

The tested specimens were designed to fail in flexure mode of failure in two groups. All slabs tested under distributed load and divided into 6 slabs reinforced by steel bars and 6 slabs reinforced by GFRP bars as a reference slabs with other parameter as dimensions, reinforcement ratio, surface texture and area of steel bar. All specimens to represent the typical flooring slab system. Table 4.1 showed the cracking load, ultimate failure load, and failure mode of the slabs. The results in Table 2 were presented for the twelve specimens. These specimens were those that were tested under Distributed load condition. The results of the slabs subjected to moment loading condition. The ultimate load carrying capacity in group I and II is presented as well in Figure 4.1 and 4.2. In the figure.

TABLE (4): Experimental results of tested slabs

| Group | Specimen | Crack load | | Ultimate | | Crack/Ultimate (%) | | Failure mode |
|-------|----------|----------------------|----------------------|---------------------|---------------------|--------------------|----------------|--------------|
| | | P _{cr} (kN) | Δ _{cr} (mm) | P _u (kN) | Δ _u (mm) | Load (%) | Deflection (%) | |
| I | S1-1 | 21.00 | 4.10 | 57.00 | 64.80 | 32.5 | 6.30 | Flexure |
| | S1-2 | 20.00 | 5.54 | 53.00 | 26.11 | 37.7 | 21.22 | Flexure |
| | S1-3 | 55.00 | 8.64 | 137.0 | 48.28 | 40.15 | 17.89 | Flexure |
| | S1-4 | 15.00 | 5.11 | 49.00 | 28.40 | 42.86 | 17.00 | Flexure |
| | S1-5 | 13.00 | 2.12 | 56.00 | 40.50 | 23.22 | 5.230 | Flexure |
| | S1-6 | 16.00 | 5.88 | 110.0 | 55.00 | 14.50 | 10.69 | Flexure |
| II | S2-1 | 77.00 | 9.27 | 170.0 | 34.51 | 45.30 | 26.86 | Flexure |
| | S2-2 | 46.00 | 5.83 | 230.0 | 44.11 | 20.00 | 13.20 | Flexure |
| | S2-3 | 108.0 | 9.22 | 372.0 | 31.40 | 29.00 | 29.36 | Flexure |
| | S2-4 | 61.00 | 4.50 | 161.0 | 24.39 | 37.89 | 18.45 | Flexure |
| | S2-5 | 32.00 | 4.42 | 124.0 | 54.30 | 25.80 | 8.14 | Flexure |
| | S2-6 | 82.00 | 6.52 | 252.0 | 39.40 | 32.54 | 16.5 | Flexure |

As show in Figure 11 and Table 4, Specimens S1-1, S1-2 and S1-3 (specimen with steel bars) had the maximum ultimate load capacity with an increase of more than 45% over that of the slabs S1-4,S1-5,S1-6 (specimen with GFRP bars). The cracking load of the specimens ranged from 15 (Specimens S1-4) to 55 kN (Specimens S1-3) with an increase of 46.4%. The cracking loads reported in Table 4.1 was the recorded load levels where the first major crack was noted.

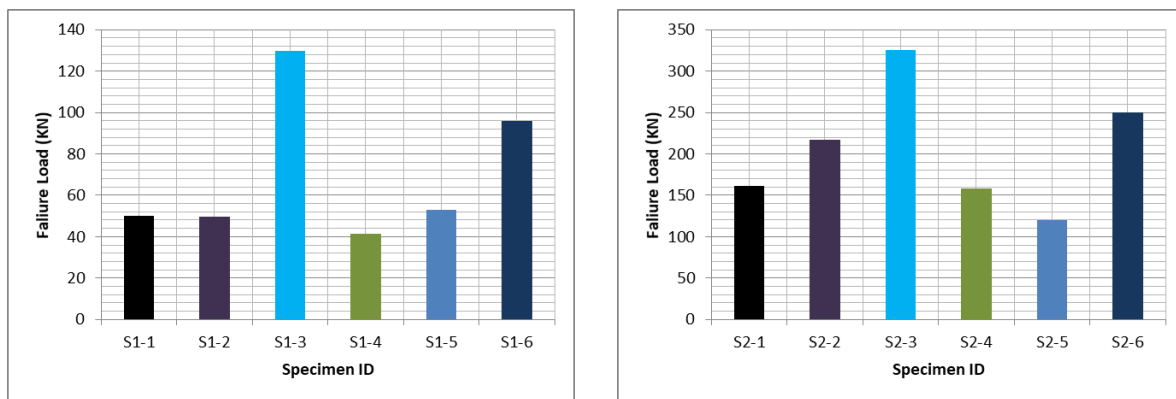


Fig 11: Experimental ultimate load carrying capacity of the specimens for Group II

In case of the specimen S1-1 as shown in figure 12 (The slab with steel reinforcement), the cracks were first initiated radially at a load level of 21 kN. With the increase of the applied load, several radial cracks initiated underneath the loading point and propagated toward the slab ends. These cracks were developed on the bottom side of the slab. Closer to the failure load, the radial cracks were dominated by a flexure cracks.



i) Bottom View Before Test



ii) Elevation View Before Test



i) Bottom View

ii) Top View

Figure (12): Crack Pattern for Specimen S1-1 (Failure Load = 57KN)

2.3 Load Deflection Curves

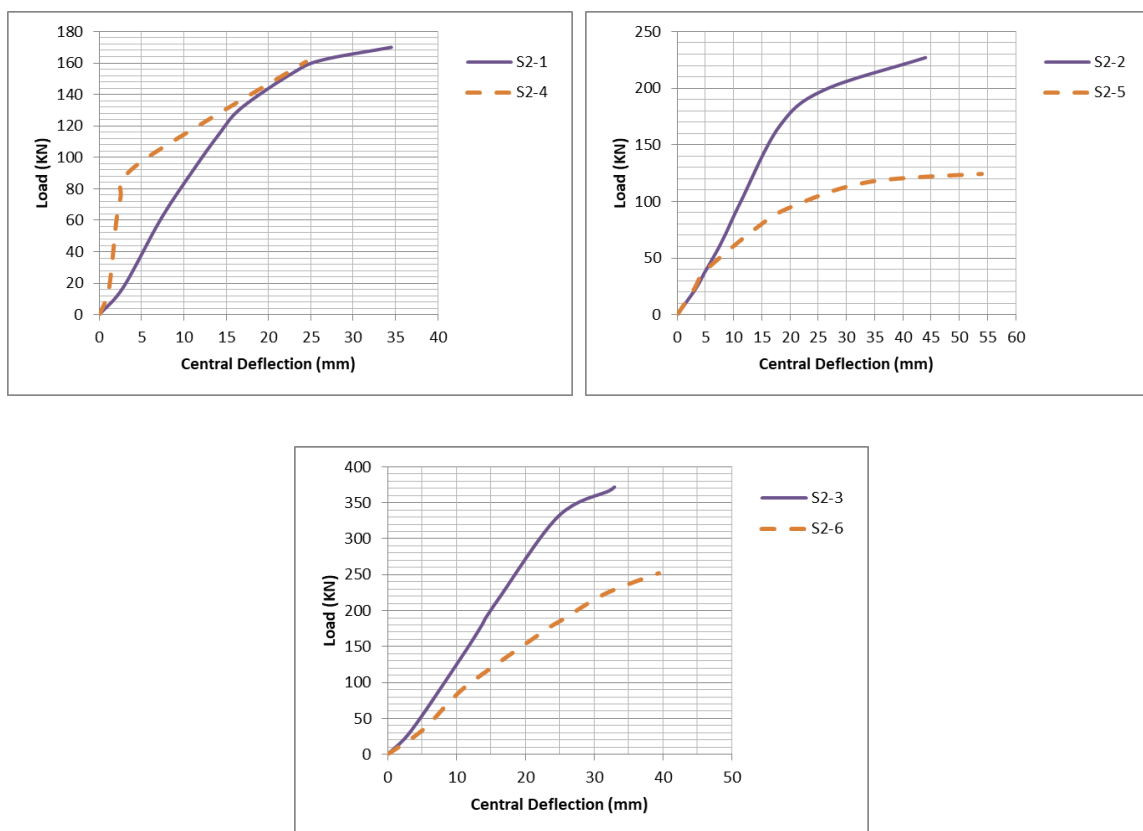


Fig 13: Load-central Deflection for Group II

Furthermore, comparing the deflection profiles of the specimens S2-1, S2-2, S2-3, S2-4, S2-5 and S2-6 were given in Figure 13, for the deflected shapes. The figures showed that the maximum deflection was recorded in the center of the specimen and it decreased as toward the supports.

III. CONCLUSION

- 1- The load deflection curve Behavior of concrete slabs reinforced with GFRP rebars up to cracking followed by an approximately was linear with lower stiffness before cracking and then a softer linear part from cracking to failure.
- 2- Comparing the failure loads of the slabs reinforced with the same cross sectional area of steel bars by GFRP rebars, there was 25% increase in the failure load of steel reinforced slabs. This increase was due to lack of dowel action of GFRP bars and low elastic modulus of GFRP bars in comparison to steel bars.

- 3- The load deflection curve behavior of concrete slabs reinforced with GFRP rebars up to cracking followed by an approximately was linear with lower stiffness before cracking and then a softer linear part from cracking to failure.
- 4- The stiffness of GFRP reinforced concrete slab was significantly lower than it for the steel sample reinforced with the same area of reinforcement after cracking, consequently, larger crack, deflection and strains. Increasing the area of the reinforcement of GFRP rebars.
- 5- Deflections of slabs reinforced with GFRP bars are significantly larger than slabs reinforced with conventional steel bars there was 30% increase in the deflection of GFRP reinforced slabs. This due to the low elastic modulus of GFRP bars in comparison to steel bars.
- 6- The result of this work, shows that light-weight concrete can be designed to meet the criteria of compressive strength of load bearing concrete and suitable solution in construction. Besides, light-weight concrete has been identified as a suitable material to replace the normal concrete. At the same time, the density of light-weight concrete can be designed and controlled according to the ratio of the mixture used.
- 7- The change of bar diameter resulting in change the failure load and small difference in deflections. This due to the change in the surface area of reinforcement.

REFERENCES

- [1] Cosenza, E, Manfredi, G., and Realfonzo, R. (1997), "Behaviour and Modeling of Bond of FRP- Rebars to Concrete", *Journal of Composites for Construction*, Vol .1, no. 2, pp. 40-51.
- [2] Deitz. D. H, HarikI. E, and Gesund. H, (1999) "One-Way Slabs Reinforced with Glass Fiber Reinforced Polymer Reinforcing Bars" *Special Publication Volume: 188*, P 279-286
- [3] Dulude.C, Ahmed. F, El-Gamal.S, (2010) "Testing of Large Scale Two Way Slabs Reinforced with GFRP bars" *The 5th international conference on FRP composite in civil Engineering*, pp.287.
- [4] Alkhrdaji, T., L. Ombres and A. Nanni, (2000) "Flexural Behavior and Design of One-Way Concrete Slabs Reinforced with Deformed GFRP Bars," *Proc., 3rd Inter. Conf. on Advanced Composite Materials in Bridges and Structures*, Ottawa, Canada, J. Humar and A.G. Razaqpur, Editors, pp. 217-224.
- [5] Nasser F. H., (2015). "Structural Behavior of Light Weight Concrete Slab Panels Reinforced with CFRP Bars." *Ph.d. Thesis of Babylon University, Babylon. March*, pp.202.
- [6] Qusai S. A., (1995). "Properties of Light Weight Concrete Made From Local Porcelenite Aggregate." *M.Sc. Thesis University of Baghdad, Baghdad, April*, pp.117.
- [7] Abbasi, M.S.A., Baluch, M.H., Azad, A.K. and Abdel-Rahman. H.H.,(2008), "Nonlinear Finite Element Modeling of Failure Modes in Reinforced Concrete Slabs", *Journal of Computers and Structures*, Vol.42, No. 5, pp. 815-823.
- [8] American Concrete Institute (ACI) State-of-the-Art Report (1999), "Provisional Design Recommendations for Concrete Reinforced with FRP Rebar's "Draft document.
- [9] Abd Elnaby, S.F. (1998), "State of the art report on the Use of fiber reinforced polymers for reinforcing concrete elements" *State of the Art Report, Faculty of Engineering, Helwan University, September 1990*, p.34
- [10] Abdallah, H., El-Badry, M, and Riskalla, S.(1996), "Behavior of concrete slabs Reinforced by GFRP", *Advanced Composite Materials, State-of-the-Art Report, The First Middle East Workshop on the Structural Composite, Ain Shams University by The Egyptian Society of Engineers. Sharm El-Sheikh. Egypt. June 1996*, PP. 229-226.
- [11] American Concrete Institute (ACI) State-of-the-Art Reporte (2006). "Fiber Reinforced plastic (FRP) Reinforced for Concrete Structures, Report by ACI Committee.440.
- [12] Benmokrane, B., Tighiouart B., Chaallal O., (1996) "Bond strength and load distribution of composite FRP rebars in concrete" *ACI Mater. J.*1996;96(3):246-53.

- [13] Benmokrane, B. and Masmoudi, R.(1996), "FRP C-bar Reinforcing Rod for concrete Structures", Advanced Composite Materials in Bridges and Structures (ACMBS-II), proceedings of the 2nd International Conference, Montreal, Quebec, Canada, pp.181-188.
- [14] Benmokrane B., Chaallal O. And Masmoudi R., (2005) "Glass Fiber Reinforced Plastic (GFRP) Rebars for Concrete Structures" Construction and Building Materials, Vol. 9, No. 6, pp. 353-364.
- [15] Bedard, Claude (1992), "Composite Reinforcing Bars: Assessing Their Use in Construction" Concrete International, Vol.14, no.1, pp.55-59.
- [16] Consenza, E., Manfredi , G., and Realfonzo, R.(1996) ,"Il Calcolo Della Lunghezza di Anchoraggio per Barre in plastic Fibro- Rinforzata (FRP)", Proceedings of the 11th Congresso CTE, Napoli, 7-9Nov. 1996, pp.451-461.